

Henryk KUCHA *, Adam PIESTRZYŃSKI *, Witold SALAMON *

GEOCHEMICAL AND MINERALOGICAL STUDY OF SULPHIDE MINERALS OCCURRING IN MAGNETITE ROCKS OF NE POLAND

UKD 549.3:552.32(438—18):550.4.08+549.08

Abstract. Pyrrhotite is the main sulphide mineral of the rocks in question. It occurs both as monoclinic Fe_7S_8 and as hexagonal variety ranging in composition from Fe_9S_{10} to $Fe_{11}S_{12}$. Smithite — $(Fe, Ni)_9S_{11}$ — containing up to 1.2 wt. % Ni was found to occur as exsolution product resulting from oxidation of monoclinic pyrrhotite. Nickel is usually connected with monoclinic pyrrhotite whilst its hexagonal variety contains very negligible amounts of this element which cannot be detected using electron microprobe method.

Pentlandite was found to occur here in two modifications: typical — low in cobalt, and abnormal — containing much Co. The oxidation of primary cobalt-bearing pentlandite resulted in its decomposition into normal pentlandite and thiospinel. This decomposition was accompanied by exsolution of mackinawite. Sometimes this process continued yielding cobaltic pyrite as final product. With decrease of temperature, pentlandite and $(Fe, Ni)(Co, Ni)_2S_4$ are locally formed as decomposition product of monosulphide solid solution rich in Cu, Ni and Co, accompanied by exsolution of talnakhite and pyritic phases.

Besides, the samples examined contained ilvaite and graphite formed during substitution of titanomagnetite by graphite-siderite association.

METHODS OF ANALYSIS

Chemical analyses of the samples were carried out by means of electron microprobe analyzer Cameca MS-46 using accelerating potential 20 kV, beam current 140 μA , sample current for free ThO_2 9.5 nA. FeS_2 , Ni, Co and As standards were used. Counting time was in the range 80 to 100 sec. Corrections for absorption of radiation and fluorescence were introduced

* Academy of Mining and Metallurgy, Institute of Geology and Mineral Deposits, Cracow (Kraków, al. Mickiewicza 30).

as well as for the difference in atomic numbers between those of standards and samples (Philbert, Tixier 1968). The precision of determinations of the main elements in the analyzed minerals was found to be, on the average, ± 1 relative per cent.

INTRODUCTION

The ore mineralization in question is connected with basic rocks of the Basement of NE Poland. It is represented by magnetite and titanomagnetite, with ilmenite, minerals of spinel-hercynite series and ulvöspinel segregations, accompanied by ilmenite and less common haematite. Ilmenite is sometimes altered into anatase. Corundum, siderite and hydrated iron oxides were also found to occur.

The above mineral association is accompanied by dispersed sulphide mineralization. The content of the latter minerals amounts to 0.5—1.5 vol. per cent, whereby sulphide concentrations are from 0.5 to 5.0 mm in size. They are generally represented by typical igneous paragenesis: pyrrhotite-pentlandite-chalcopyrite. Microscope examinations have shown that the above minerals are accompanied by pyrite, marcasite, mackinawite, cubanite and, locally, graphite which was also observed by Siemiątkowski (1976).

RESULTS

Pyrrhotite

This is the commonest sulphide mineral, occurring in two generations. The first of them is much more widespread and coexists with chalcopyrite and octahedral pentlandite or occurs as separate, usually polycrystalline aggregates. When examined using immersion technique, these grains display polysynthetic twinning and, often, lamellar structures resulting from decomposition of solid solutions which are particularly distinct if observed on etched surfaces. They are, most probably, decomposition products of high-temperature pyrrhotite in $T-X$ system into its low-temperature hexagonal + monoclinic modifications or monoclinic pyrrhotite + smithite $(\text{Fe}, \text{Ni})_9\text{S}_{11}$ (Fig. 1). Moreover, pyrrhotite of the first generation often contains flame-shaped pentlandite inclusions reported for numerous ore deposits (Ramdohr 1960, Taylor and Williams 1972). As follows from microprobe analytical data (Table 1), the composition of pyrrhotite of this generation varies from $\text{Fe}_{0.75}\text{S}$ to $\text{Fe}_{0.93}\text{S}_{1.00}$, corresponding to typical low-temperature hexagonal pyrrhotite (Fe_9S_{10} , $\text{Fe}_{10}\text{S}_{11}$, $\text{Fe}_{11}\text{S}_{12}$ — Bennet *et al.* 1972). The intermediate phases are represented by $(\text{Fe}, \text{Ni})_{0.82}\text{S}_{1.00}$ (smithite $(\text{Fe}, \text{Ni})_9\text{S}_{11}$ Taylor and Williams 1972), $\text{Fe}_{0.88}\text{S}_{1.00}$ (typical monoclinic pyrrhotite Fe_7S_8) and $\text{Fe}_{0.90}\text{S}_{1.00}$ — $\text{Fe}_{0.91}\text{S}_{1.00}$. The commonest are compositions ranging between $(\text{Fe}, \text{Ni})_{0.82}\text{S}_{1.00}$ and $(\text{Fe}, \text{Ni})_{0.88}\text{S}_{1.00}$, corresponding to monoclinic pyrrhotite and smithite mixtures. Those corresponding to greigite ($\text{Fe}_{0.75}\text{S}$ — Skinner *et al.* 1964) are very scarce.

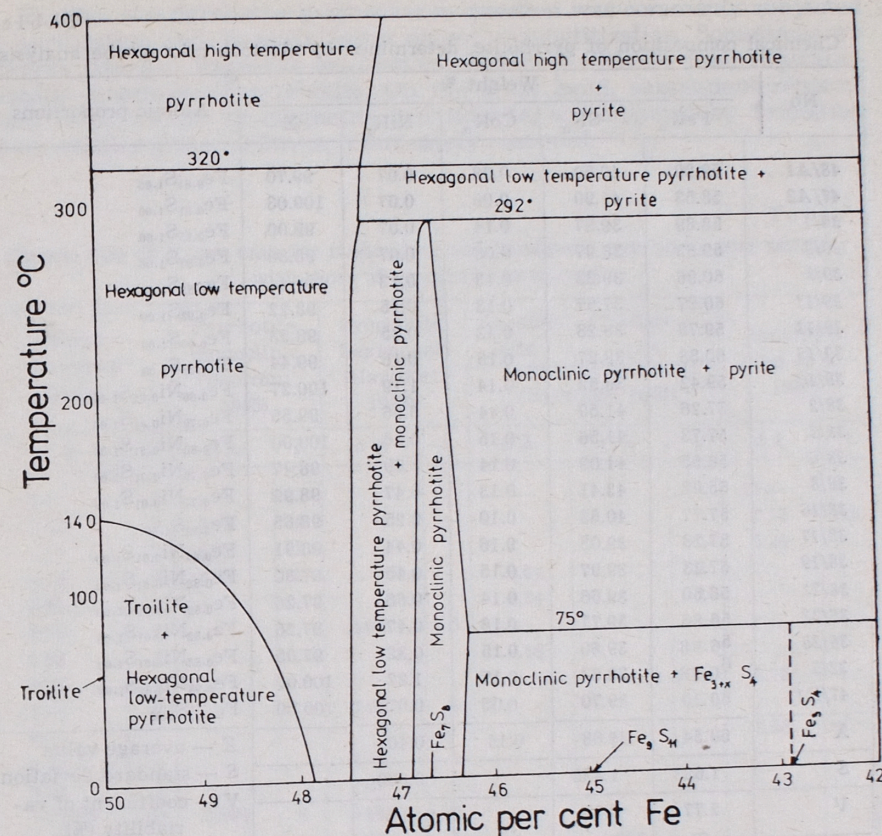


Fig. 1. A part of the Fe-S system at low temperature (after Taylor 1970, modified after Kullerud 1968). All phases coexist with vapour

The majority of the results is situated in the field limited by compositions Fe_7S_8 and Fe_9S_{11} and by temperature 75°C , corresponding to stability limit of smithite (Taylor 1970, Fig. 1). This corresponds to decomposition of nickel-rich pyrrhotite into Fe_7S_8 and $(\text{Fe}, \text{Ni})_9\text{S}_{11}$ (smithite). It is supposed that the grains showing compositions ranging from $\text{Fe}_{0.88}\text{S}_{1.00}$ to $\text{Fe}_{0.90}\text{S}_{1.00}$ correspond to submicroscopic intergrowths of hexagonal and monoclinic pyrrhotites, situated in low-temperature field of this mixture (Fig. 1). The Fe : S ratio exceeding 0.90 corresponds to the stability field of low-temperature hexagonal pyrrhotite whilst 0.93 — enters the field of troilite + low-temperature hexagonal pyrrhotite. The latter case could correspond to microscopically observed intergrowths of hexagonal pyrrhotite and Ni-bearing mackinawite. Hexagonal structure of the latter pyrrhotite was revealed after etching using saturated chromate mixture (Bennet *et al.* 1972).

X-ray investigations have confirmed the conclusions resulting from chemical data (Table 2). The above described first generation of pyrrhotite

Table 1

Chemical composition of pyrrhotite, determined by electron microprobe analysis

No	Weight %					Atomic proportions
	FeK _α	SK _α	CoK _α	NiK _α	Σ	
48/A1	59.20	40.50	0.08	0.07	99.70	Fe _{0.84} S _{1.00}
47/A2	58.53	41.90	0.08	0.07	100.03	Fe _{0.81} S _{1.00}
39/1	58.89	39.97	0.14	0.07	99.00	Fe _{0.85} S _{1.00}
39/2	59.83	38.97	0.08	0.07	98.80	Fe _{0.88} S _{1.00}
39/8	60.96	39.23	0.13	0.12	100.44	Fe _{0.89} S _{1.00}
39/11	60.27	37.67	0.13	0.15	98.22	Fe _{0.93} S _{1.00}
39/13	59.78	38.28	0.12	0.35	98.53	Fe _{0.90} S _{1.00}
39/15	60.83	38.27	0.16	0.18	99.44	Fe _{0.91} S _{1.00}
39/16	59.42	39.52	0.14	1.19	100.27	Fe _{0.86} Ni _{0.02} S _{1.00}
38/2	57.26	41.59	0.14	0.56	99.55	Fe _{0.79} Ni _{0.01} S _{1.00}
38/3	57.73	41.56	0.15	0.56	100.00	Fe _{0.80} Ni _{0.01} S _{1.00}
38/6	56.55	41.09	0.14	0.69	98.47	Fe _{0.79} Ni _{0.01} S _{1.00}
38/8	55.98	43.41	0.13	0.47	98.99	Fe _{0.74} Ni _{0.01} S _{1.00}
38/16	57.77	40.63	0.10	0.25	98.65	Fe _{0.82} S _{1.00}
38/17	57.28	39.03	0.16	0.44	96.91	Fe _{0.84} Ni _{0.01} S _{1.00}
38/19	57.23	39.97	0.15	0.45	97.80	Fe _{0.82} Ni _{0.01} S _{1.00}
38/21	56.80	39.66	0.14	0.66	97.26	Fe _{0.82} Ni _{0.01} S _{1.00}
38/23	56.86	39.77	0.16	0.47	97.26	Fe _{0.82} Ni _{0.01} S _{1.00}
38/25	56.88	39.60	0.15	0.32	97.05	Fe _{0.88} Ni _{0.01} S _{1.00}
32/5	60.98	38.63	0.17	1.22	100.00	Fe _{0.93} Ni _{0.02} S _{1.00}
47/B1	60.30	39.70	0.08	0.07	100.00	Fe _{0.87} S _{1.00}
X	58.54	39.88	0.13	0.40		X — average value
S	1.623	1.425		0.338		S — standard deviation
V	2.77	3.57		84.50		V — coefficient of variability (%)

was found to consist of both low-temperature modifications and smithite. Since larger (Fe, Ni)₉S₁₁ grains are scarce, the presence of smithite is manifested by the existence of submicroscopic or similarly small segregations of this mineral within monoclinic pyrrhotite. This explains their intermediate composition between Fe₇S₈ and (Fe, Ni)₉S₁₁. Similar phenomena were often observed by Bennet *et al.* (1972) who observed lamellar intergrowths of monoclinic pyrrhotite and smithite, or submicroscopic exsolution forms of smithite (pentlandite, violarite) located at the boundary of twin grains or of magnetic domain structures.

The observed fairly considerable differences in composition of pyrrhotite of the first generation can be explained by assuming that after liquation of silicate-oxide and sulphide melts, the latter was closed within isolated spaces limited by non-sulphide minerals occurring in various proportions. As follows from experimental data (Kullerud 1968), considerable variations of Fe : S proportions could take place on cooling due to reactions of sulphides with surrounding silicate phases. These processes were accompanied by low-temperature oxidation resulting in the formation of smithite.

Besides, the pyrrhotite generation in question was commonly subjected to pyritization and, to much lesser extent, magnetitization. Sometimes we observe lamellar magnetite oriented concordantly with the main crystallographic directions of pyrrhotite. On the other hand, subsequent replacement of pyrrhotite by magnetite and siderite, accompanied by formation of vermicular graphite forms, is but rarely observed.

Table 2

Comparison of X-ray data for monoclinic and hexagonal pyrrhotite and smithite with those of pyrrhotite examined

Sample examined CoK _α	Pyrrhotite monoclinic (Bystrom 1945)		Pyrrhotite hexagonal (Harcourt 1942)		Pentlandite (Harcourt 1942)			Chalkopyrite		Smythite (Erd <i>et al.</i> 1957)	
	d Å	I	d Å	I	d Å	d Å	I	d Å	I	d Å	I
9.8	1									11.5	6
5.86	3	5.75	4							5.75	0.5
5.27	2	5.29	2							5.29	2
4.73	3	4.72	2			3.54		2			
3.38 b	1					3.34		2			
3.00	7			2.97	6						
2.88	3					2.89		7			
2.75	2									2.75	4
2.65	9			2.63	8					2.56	6
2.55	1										
2.46	4			2.45	1						
2.25	2			2.26	1						
2.066 b	10	2.067	8	2.062	10						
1.87	4			1.88	1						
1.78	1					1.77	1.855	10			
1.751	1							10			
1.722	8			1.718	7						
1.659	1									1.672	4
1.609 d	3	1.603	4	1.612	4						
1.566	4	1.593	4				1.586	10			
1.469	2									1.468	0.5
1.443	5	1.440	2								
1.425	4	1.422	6	1.428	5						

b — broad,
d — diffuse.

The second generation of pyrrhotite appears locally in siderite-graphite association replacing metasomatically primary titanomagnetite. Spinel and ilmenite grains thus formed preserve within titanomagnetite pseudomorphs their primary position and only ilmenite displays oxidation to titanium oxides. These processes are accompanied by exsolution of graphite and, locally, ilvaite.

Smithite (Fe,Ni)₉S₁₁

Larger scarce smithite crystals show typical optical properties (Nickel and Harris 1971) i.e. display high reflectivity (42%) and distinctly higher polishing hardness. Chemical composition determined by electron microprobe method (Table 3) corresponds to the formula proposed by Taylor

Table 3

Chemical composition of smithite determined by electron microprobe analysis

No	Weight %				Σ	Atomic proportions
	FeK _α	SK _α	CoK _α	NiK _α		
39/16	59.42	39.52	0.14	1.19	100.27	Fe _{0.86} Ni _{0.02} S _{1.0}
38/3	57.73	41.73	0.15	0.56	100.00	Fe _{0.80} Ni _{0.01} S _{1.0}
38/19	57.23	39.97	0.15	0.45	97.80	Fe _{0.82} Ni _{0.01} S _{1.0}
38/21	56.80	39.66	0.14	0.66	97.26	Fe _{0.82} Ni _{0.01} S _{1.0}
38/23	56.86	39.77	0.16	0.47	97.26	Fe _{0.82} Ni _{0.01} S _{1.0}

and Williams (1972) i.e. to (Fe,Ni)₉S₁₁ but not to Fe₃S₄ as suggested by Erd *et al.* (1957). Two generations of smithite were found in samples under study. The first one is represented by crystals up to 0.X mm in size or occurs as submicroscopic segregations at the boundaries of lamellae and of magnetic domain structures in monoclinic pyrrhotite. The second generation was formed due to oxidation processes connected with replacement of pyrrhotite by magnetite-siderite-graphite paragenesis.

As follows from chemical data obtained, nickel is connected either with smithite or with monoclinic pyrrhotite-smithite intergrowths.

Pentlandite — M₃S₄ — MS₂ series

This mineral is much less common than pyrrhotite, forming paragenetic intergrowths with the latter, as well as with chalcopyrite and, sometimes, cubanite. It is usually accompanied by mackinawite. Two varieties of pentlandite were distinguished on the ground of microscope studies. The first one displays typical optical properties of (Fe, Ni)₉S₈, though contains several per cent of cobalt (Table 4). The second variety, called *cobalt-rich pentlandite* (Phot. 1) exhibits pink colouration, distinctly higher polishing hardness and does not show typical pentlanditic cleavage. This modification is developed in the form of irregular system of veinlets and lamellae within normal pentlandite grains (Phot. 1 and 3). Exsolution process of *cobalt-rich pentlandite* from primary (Fe, Ni, Co)₉S₈ is accompanied by the formation of mackinawite. Decomposition structures of pentlandite and M₃S₄ in talnakhite and mooihoekite were found too.

The M : S ratio in pentlandites under study varies from 0.70 to 1.19 (Table 5) i.e. considerably exceeds the reported data for natural pentlandites (0.90—1.20, Knap *et al.* 1965). Such deficiency of cations, when compared with the formula M₉S₈, cannot be explained in terms of normal

Table 4

Chemical composition of pentlandite and its decomposition product — thiospinel electron microprobe data

No	Weight %				Σ	Atomic proportions (Fe _x Co _y Ni _z) _{x+y+z}
	FeK _α	SK _α	NiK _α	CoK _α		
32/1	23.86	33.00	33.13	7.62	97.61	(Fe _{3.32} Co _{1.01} Ni _{3.25}) _{7.58} S _{8.00}
32/1'	11.87	36.26	25.30	23.74	97.17	(Fe _{1.50} Co _{2.85} Ni _{3.05}) _{7.40} S _{8.00}
32/2	13.78	36.93	27.95	19.11	97.77	(Fe _{1.71} Co _{2.25} Ni _{3.31}) _{7.27} S _{8.00}
32/3	28.43	31.92	34.77	4.88	100.00	(Fe _{4.09} Co _{0.87} Ni _{4.76}) _{9.52} S _{8.00}
32/4	12.34	38.95	25.69	21.65	98.23	(Fe _{1.47} Co _{2.44} Ni _{2.91}) _{6.82} S _{8.00}
38/1	7.00	43.46	21.08	28.40	100.00	(Fe _{0.74} Co _{2.85} Ni _{2.12}) _{5.71} S _{8.00}
38/5	13.40	41.43	28.46	15.04	98.33	(Fe _{1.49} Co _{1.55} Ni _{3.01}) _{6.05} S _{8.00}
38/15	29.42	34.80	28.87	5.81	98.90	(Fe _{3.88} Co _{0.73} Ni _{3.63}) _{8.24} S _{8.00}
38/18	28.53	33.72	29.47	7.11	98.83	(Fe _{3.89} Co _{0.92} Ni _{3.82}) _{8.63} S _{8.00}
38/20	27.99	33.97	29.40	7.02	98.38	(Fe _{3.79} Co _{0.90} Ni _{3.78}) _{8.47} S _{8.00}
38/22	29.56	34.13	30.21	6.16	100.06	(Fe _{3.95} Co _{0.79} Ni _{3.77}) _{8.54} S _{8.00}
38/24	29.60	31.13	29.02	6.86	96.61	(Fe _{4.37} Co _{0.96} Ni _{4.08}) _{9.41} S _{8.00}
39/17	31.52	33.46	28.61	5.96	99.55	(Fe _{4.33} Co _{0.78} Ni _{3.74}) _{8.85} S _{8.00}
39/18	32.22	36.09	27.08	4.58	99.97	(Fe _{4.01} Co _{0.55} Ni _{3.29}) _{7.84} S _{8.00}
40/2	10.31	42.19	23.22	20.92	96.64	(Fe _{1.12} Co _{2.16} Ni _{2.41}) _{5.69} S _{8.00}
40/3	28.24	34.49	35.07	1.87	99.67	(Fe _{3.76} Co _{0.24} Ni _{4.44}) _{8.44} S _{8.00}
40/4	16.92	43.90	23.71	14.83	99.36	(Fe _{1.77} Co _{1.47} Ni _{2.36}) _{5.60} S _{8.00}
40/5	22.59	37.17	29.40	8.33	97.49	(Fe _{2.79} Co _{0.98} Ni _{3.46}) _{7.23} S _{8.00}
40/6	11.11	41.90	22.70	22.77	98.48	(Fe _{1.22} Co _{2.37} Ni _{2.37}) _{5.96} S _{8.00}
<i>x</i>	21.51	36.76	28.06	12.24	98.38	<i>x</i> — average value,
<i>s</i>	8.71	4.32	3.84	8.12		<i>s</i> — standard deviation,
<i>v</i>	40.51	11.84	13.70	66.35		<i>v</i> — coefficient of variability (%).

pentlandite structure. The ratio M : S = 9 : 8 (Table 4 (32/3, 38/24) can be due to the presence of heazlewoodite admixture (Kullerud 1968). According to Knap's *et al.* (1965) data, the M : S ratios up to 7.2 : 8 can be considered as attributable to pentlandite. However, further decrease of this ratio (Table 4 and 5) can be explained only by assuming the presence of thiospinel phases. This is particularly distinct in the analysis 38/5 (Table 4), corresponding exactly to the formula M₃S₄.

Further decrease of the discussed ratio (38/1, 40/2, 40/4 — Table 4) suggests the presence of phases of MS₂ type. All the analyses in question were carried out within microscopically light-pinkish exsolutions showing distinctly higher hardness than formed simultaneously thiospinel phases. It should be also emphasized that these inclusions of hard mineral are regular in shape what is characteristic of the phases of MS₂ type. All the minerals in question do not contain determinable amounts of arsenic (using microprobe technique).

Geochemical relations between sulphur and metallic elements during transformations of M₉S₈ into M₃S₄ were investigated by means of correlation analysis of data on pentlandite population examined (Table 6). Nega-

Table 5

Fe : Ni, Fe : Co, (Fe + Ni) : Co, M : S ratios and the values of spinel coefficient t pentlandites and their decomposition products

No	Fe : Ni	Fe : Co	(Fe + Ni) : Co	M : S	t
32/1	1.02	3.29	6.50	0.95	0.4733
32/1'	0.49	0.53	1.59	0.93	0.5333
32/2	0.52	0.76	2.23	0.91	0.5766
32/3	0.86	6.10	13.21	1.19	-0.1733
32/4	0.50	0.60	1.79	0.85	0.7267
38/1	0.35	0.26	1.00	0.71	1.0966
38/5	0.49	0.94	2.85	0.76	0.9733
38/15	1.07	5.31	10.29	1.03	0.2533
38/18	1.02	4.22	8.38	1.08	0.1233
38/20	1.00	4.21	8.41	1.06	0.1767
38/22	1.05	5.04	9.81	1.07	0.1533
38/24	1.07	4.85	8.80	1.18	-0.1367
39/17	1.15	5.55	10.35	1.11	0.0500
39/18	1.22	7.29	13.25	0.98	0.3867
40/2	0.46	0.52	1.63	0.71	1.1033
40/3	0.85	15.67	34.17	1.06	0.1867
40/4	0.76	1.20	2.81	0.70	1.1333
40/5	0.81	2.85	6.37	0.90	0.2567
40/6	0.51	0.51	1.51	0.75	1.0133

Table 6

Linear correlation coefficients and parameters of regression lines calculated for pentlandite population examined and for M_3S_4

Correlation	r	a	b
Fe—S	-0.793	45.054	-0.394
Fe—Ni	0.673	21.305	0.314
Fe—Co	-0.958	31.447	-0.893
Ni—Co	-0.819	60.809	-1.731
Co—S	0.735	31.776	0.392
Ni—S	-0.818	62.439	-0.922
t —Fe	-0.862	29.722	-17.514
t —S	0.670	33.413	6.761
t —Ni	-0.770	31.303	-6.909
t —Co	0.798	5.161	15.119

t — spinel coefficient,

r — linear correlation coefficient,

$y = a + bx$ — equation of regression line,

$(x + y + z) = M_3S_4t + M_3S_4(1 - t)$.

negative correlation coefficients M—S for Fe and Ni and positive for Co (Table 6) indicate that exsolution of thiospinel phase from pentlandite is determined by high Co content. This conclusion is confirmed by positive values of correlation coefficients only for the pairs t —S and t —Co. As follows from

these data, during decomposition of pentlandite accompanied by exsolution of mackinawite nearly all the Co present is incorporated into M_3S_4 whilst the majority of Ni enters into mackinawite (Table 8). As follows from comparison of correlation coefficients and of parameters of regression line (Table 6), Fe and Ni tend, in the presence of Co, to occur in the divalent form. This tendency is expressed much more distinct by Fe and Ni, both in the presence of Co and relative to spinel coefficient. Divalent form of iron is also favoured in the presence of Ni (Table 6). It is thus concluded that the formula of thiospinel exsolved from pentlandite can be expressed as follows: $(Fe, Ni)(Co, Ni)_2S_4$. Consequently, iron is supposed to occur in divalent form, cobalt mainly as Co^{3+} whilst nickel both as Ni^{2+} and Ni^{3+} . This corresponds to a mixture of thiospinels $FeCo_2S_4$, $NiCo_2S_4$ and $FeNiS_4$. Taking into account the distribution of cations in thiospinel structures (Table 7) and the results of regression analysis (Table 6) it is concluded that Co occurs mainly in octahedral positions, Ni — both in octahedral and tetrahedral ones whilst Fe enters essentially tetrahedral sites of spinel structure.

Table 7

Observed distribution of cations in thiospinels and pentlandites

Compound	Octahedral site	Tetrahedral site	Authors
$FeCo_2S_4$	$2Co^{3+}$ (?)	Fe^{2+} (?)	Rajamani and Prewitt 1975
$CoCo_2S_4$	$2Co^{3+}$	Co^{2+}	Vaughan <i>et al.</i> 1971
$NiCo_2S_4$	$2Co^{3+}$	Ni^{2+}	Knop <i>et al.</i> 1968
$FeNi_2S_4$	$Fe^{2+} + Ni^{3+}$	Ni^{3+}	Vaughan <i>et al.</i> 1971
$NiFe_2S_4$	$Ni^{2+} + Fe^{3+}$	Fe^{3+}	Vaughan <i>et al.</i> 1971
$NiCo_8S_8$	Co + Ni	Co + Ni	Knop, Ibrahim 1961
$(Fe, Ni)_3S_8$	$3/4 Fe + 1/4 Ni$	Fe + Ni	Knop <i>et al.</i> 1970

The commonest mechanism of formation of thiospinel consists in decomposition of pentlandite into Ni-mackinawite + pentlandite + $(Fe, Ni)(Co, Ni)_2S_4$. The latter mineral sometimes alters into cobalt-rich pyrite. This oxidation series corresponds to that of pyrrhotite which was described previously.

It is supposed that there is another, less common, mode of formation of thiospinel. It consists in decomposition of monosulphide solid solution, enriched in Cu, Ni and Co into talnakhite (mooihoekite) + pentlandite + $(Fe, Ni)(Co, Ni)_2S_4$. Because of coexistence of pentlandite and pyrite-like phase this decomposition is possible at temperature below $300^\circ C$ (Kullerud 1968). This process is but rarely observed microscopically, being not accompanied by segregation of mackinawite.

Mackinawite

This mineral is usually associated with pentlandite, being less common among decomposition products of pyrrhotite. In the latter case it occurs at

the boundaries of pyrrhotite and haycockite crystals. In general, it forms lamellar exsolution products resulting from decomposition of cobalt-rich pentlandite and consisting of Ni-mackinawite, pentlandite and thiospinel. Usually mackinawite is rich in Ni and low in Co (Table 8). This confirms our earlier conclusion that M^{+3} positions in thiospinel are occupied essentially by Co^{+3} and to lesser extent by Ni^{+3} whilst iron occurs mainly in divalent form.

Table 8

Comparison of chemical composition of mackinawite from magnetite rocks in NE Poland with those from S Africa and Finland

Locality	Weight %					Formula
	Fe	Co	Ni	S	Me	
Vlakfontein South Africa	38.1	3.3	18.7		60.1	
Transval * Outukumpu, Finland	52.0	5.9	1.8		59.7	
Outukumpu, Finland **	53.1 ± 2	0.2	5.4 ± 0.3		58.7	
Ylöjäevi, Finland	63.2 ± 2	0.2	0.2		63.7	
	56.74	3.0	3.55	35.03	63.29	$(Fe_{0.98}Co_{0.05}Ni_{0.05})_{1.03}S_{1.0}$
Magnetite rocks from NE Poland	41.63	5.0	16.64	35.60	63.17	$(Fe_{0.67}Co_{0.06}Ni_{0.26})_{1.01}S_{1.0}$

* After Vaughan (1969).

** After Kouvo, Vuorolainen and Long (1963).

Another type of mackinawite is connected with hexagonal pyrrhotite. It contains up to 17 wt. % Ni and up to 5 wt. % Co. Its origin can be connected with decomposition of Ni-rich hexagonal pyrrhotite in the stability field of low-temperature hexagonal pyrrhotite and troilite (Fig. 1). Mackinawite often contains minute pentlandite inclusions. This transformation would proceed at temperature below 170°C which is the upper stability limit of mackinawite (Takeno *et al.* 1970). During this process nearly total amount of Ni and Co, liberated from pyrrhotite would enter mackinawite structure. This decomposition could be contemporaneous with previously described process of decomposition of cobalt-rich pentlandite.

When examined using ore microscope, mackinawite displays strong bireflection ranging from grey to pinkish-yellow-gray in air. Its reflectivity is higher than that of mackinawite from Singhbun (Sarkar 1971) and similar to this reported by Vaughan (1969) i.e. amounts to 45—25%. Polishing hardness of mackinawite in question is slightly lower than that of pyrrhotite and higher than that of cubanite and haycockite. This is not in accordance with the data of Kuovo *et al.* (1963). Similarly, nickel-rich mackinawite from Vlakfontein (Vaughan 1969) seems to show lower hardness, no matter of rather close optical properties and chemical composition. This

may be due to higher Co content in our mackinawite when compared with that of Vlakfontein (Table 8). Polishing hardness of the latter would be similar to that of Singhbun (Sarkar 1971), showing slightly different colouration. Consequently, the hardness of mackinawite depends on its chemical composition (Vaughan 1969, Clark 1970). In this respect the mineral under examination is most similar to that of Vlakfontein (Table 8), no matter of very high Co content in the former.

Cobaltiferous pyrite

Pyrite is widespread in sulphide associations in question, though occurs in rather subordinate amounts. It forms two generations. The older is represented by isolated medium-crystalline aggregates. Some grains display zonal structure, manifested by variable hardness and colour. When compared with pure FeS_2 , cobaltiferous pyrite shows lower reflectivity and hardness. Besides, it exhibits distinct brown-orange colouration, being much less common than normal pyrite.

The second generation is connected mainly with pyritization of pyrrhotite. This process developed at the boundaries of grains and along fractures in pyrrhotite. Secondary pyrite, associated with siderite and graphite and replacing titanomagnetite was also observed.

Table 9

Chemical composition of pyrites from NE Poland determined by electron microprobe analysis

No	Weight %				Σ	Atomic proportions
	FeK _α	SK _α	NiK _α	CoK _α		
39/3	47.42	53.07	0.07	0.09	100.49	$Fe_{1.08}S_{2.0}$
39/5	42.84	52.27	1.08	3.00	99.19	$Fe_{0.94}Co_{0.06}Ni_{0.02}S_{2.0}$
39/10	46.67	53.99	0.20	0.13	100.99	$Fe_{0.99}(Ni, Co)_{0.01}S_{2.0}$
38/7	46.05	51.94	0.42	0.11	98.52	$Fe_{1.02}(Ni, Co)_{0.01}S_{2.0}$
38/10	44.40	55.00	0.07	0.55	99.95	$Fe_{0.98}Co_{0.01}S_{2.0}$
38/11	44.37	56.53	0.07	0.14	101.04	$Fe_{0.90}S_{2.0}$
38/12	41.38	54.75	0.07	2.46	98.59	$Fe_{0.87}Co_{0.05}S_{2.0}$
38/14	39.90	52.87	0.07	5.51	98.28	$Fe_{0.87}Co_{0.11}S_{2.0}$
\bar{x}	44.13	53.80	0.256	1.499	99.68	\bar{x} — average value,
s	1.599	1.560		1.516		s — standard deviation,
v	3.62	2.90		101.13		v — coefficient of variability (%).

In general, pyrite contains more Co than Ni (Table 9). Sometimes we observe a deficiency of cations relative to sulphur content. This may be due to incomplete filling of cationic positions during transformation of thiospinel lattice into pyritic one, accompanied by removal of nickel outside reacting minerals. Such interpretation results from distinct deficiency of nickel in analyzed pyrites when compared with Ni content in thiospinel.

SUMMARY

Characteristic decomposition series were found to occur in sulphide associations examined. In general they are connected with oxidation under moderate temperature conditions.

Pyrrhotite. There are two decomposition series originated from high-temperature hexagonal pyrrhotite (hex *hTpo*), rich in nickel and low in cobalt:

— Ni hex *hTpo* → Ni-mackinawite + hex low-temp pyrrhotite,

— Ni hex *hTpo* → monoclinic pyrrhotite + smithite → Ni greigite (and other possible thiospinels).

Pentlandite. In this case two decomposition series were also found to occur. The first of them would be connected with monosulphide solid solution (MSS) rich in Cu, Ni and Co and the second — with oxidation of cobaltiferous pentlandite:

— Cu, Ni, Co — MSS → talnakhite (mooihoekite, haycockite) + pentlandite + (Fe, Ni) (Co, Ni)₂S₄ + (Fe, Co)S₂,

— Co-pentlandite → pentlandite + Ni-mackinawite + (Fe, Ni) (Co, Ni)₂S₄.

Co-pyrite. This mineral is probably the product of sulphurization of thiospinel accompanied by removal of Ni.

REFERENCES

- BENNET C. E. G., GRAHAM J. and THORNBUR M. R., 1972: New observations on natural pyrrhotite. Part I. Mineralogical techniques. *Amer. Miner.* 57, 445—462.
- BYSTRÖM A., 1945: Monocline magnetic pyrites. *Ark. Kemi.* 19B, 8.
- CLARK A. H., 1970: Nickelian mackinawite from Vlaktefontein, Transvaal: a discussion. *Amer. Miner.* 55, 1802—1807.
- ERD R. C., EVANS H. T., RICHTER H. D., 1957: Smythite, a new iron sulfide and associated pyrrhotite from Indiana. *Amer. Miner.* 42, 309—333.
- HARCOURT G. A., 1942: Tables for the identification of ore minerals by X-ray patterns. *Amer. Miner.* 27, 63—113.
- KNOP O., IBRAHIM M. A., 1961: Chalcogenides of the transition elements. II. Existence of the π phase in the M₉S₈ section of the system Fe-Co-Ni-S. *Can. J. Chem.* 39, 297—317.
- KNOP O., IBRAHIM M. A., SUTARNO, 1965: Chalcogenides of the transition elements. IV. Pentlandite, a natural π phase. *Can. Miner.* 8, 291—324.
- KNOP O., REID K. I. G., SUTARNO, NAKAGAWA Y., 1968: Chalcogenides of the transition elements. VI. X-ray, neutron, and magnetic investigation of the spinels Co₃O₄, NiCo₂O₄, Co₂S₄, and NiCo₂S₄. *Can. J. Chem.* 46, 3463—3476.
- KNOP O., CHUNG-HSI HUANG, WOODHAMS F. W., 1970: Chalcogenides of the transition elements. VII. A Mössbauer study of pentlandite. *Amer. Miner.* 55, 1115—1130.
- KULLERUD G., 1968: Sulfide studies. Research in Geochemistry. *Abelson Ed.* 2, 286—321.
- KOUVO O., VUORELAINEN Y., LONG J. V. P., 1963: A tetragonal iron sulfide. *Amer. Miner.* 48, 511—524.
- NICKEL E. H., HARRIS D. C., 1971: Mineralogical notes. Reflectance and microhardness of smythite. *Amer. Miner.* 56, 1464—1469.
- PHILBERT J., TIXIER R., 1968: Electron penetration and the atomic number correction in electron probe microanalysis. *Brit. J. Appl. (J. Phys. D.)*, ser. 2, 1, 685—694.

- RAJAMANI V., PREWITT C. T., 1975: Thermal expansion of the pentlandite structure. *Amer. Miner.* 60, 39—48.
- RAMDOHR P., 1960: Die Erzminerale und ihre Verwachsungen. 3. Aufl. Berlin.
- SARKAR S. C., 1971: Mackinawite from the sulfide ores of the Singhbhum copper belt, India. *Amer. Miner.* 56, 1312—1318.
- SIEMIATKOWSKI J., 1976: Graphite in rocks of norite-anortosite Suwałki intrusion. *Prz. geol.* 4, 212—213. (in Polish).
- SKINNER B. J., ERD R. C., GRIMALDI F. S., 1964: Greigite, the thio-spinel of iron, a new mineral. *Amer. Miner.* 49, 543—555.
- TAKENO S., ZOKA H., NIHARA T., 1970: Metastable cubic iron sulfide — with special reference to mackinawite. *Amer. Miner.* 55, 1639—1649.
- TAYLOR L. A., 1970: Low-temperature phase relations in the Fe-S system. Carnegie Inst. Washington Year Book 68, 259—270.
- TAYLOR L. A., WILLIAMS K. L., 1972: Smythite, (Fe, Ni)₉S₁₁ — a redefinition. *Amer. Miner.* 57, 1571—1577.
- VAUGHAN D. J., 1969: Nickelian mackinawite from Vlaktefontein, Transvaal. *Amer. Miner.* 54, 1190—1193.
- VAUGHAN D. J., BURNS R. G., BURNS V. M., 1971: Geochemistry and bonding of thiospinel minerals. *Geochim. Cosmochim. Acta* 35, 365—381.

Henryk KUCHA, Adam PIESTRZYŃSKI, Witold SALAMON

BADANIA GEOCHEMICZNO-MINERALOGICZNE MINERAŁÓW SIARCZKOWYCH ZE SKAŁ MAGNETYTOWYCH PÓLNO-CNO-WSCHODNIEJ POLSKI

Streszczenie

Głównym minerałem siarczkowym w omawianych utworach jest pirotyt. Występuje zarówno w odmianie jednoskośnej Fe₇S₈ jak i heksagonalnej o składzie od Fe₉S₁₀ do Fe₁₁S₁₂. Ponadto stwierdzono obecność smythitu (Fe, Ni)₉S₁₁ zawierającego do 1,2% wag. Ni i wydzielającego się w procesie utleniania pirotynu jednoskośnego. Obecność niklu związana jest najczęściej z pirotynem jednoskośnym, natomiast w odmianach odpowiadających składem atomowym pirotynowi heksagonalnemu zawartość Ni jest z reguły mniejsza od granicy wykrywalności na mikroskondzie elektronowej.

Pentlandyt występuje w dwóch odmianach: typowej — z małą domieszką kobaltu i anomalnej — z wysoką zawartością Co. Pierwotnie istniejący pentlandyt kobaltowy wskutek utlenienia rozpadł się na pentlandyt normalny i thiospinel. Rozpad ten połączony jest z wydzielaniem się mackinawitu. Niekiedy końcowym wynikiem procesu utleniania jest utworzenie się piryty kobaltowego. Pentlandyt i (Fe, Ni)₁(Co, Ni)₂S₄ mogą też powstać w wyniku rozpadu (przy spadku temperatury) roztworu stałego monosiarczku bogatego w Cu, Ni i Co. Proces ten połączony jest z wydzielaniem się talnakhitu i faz odpowiadających pirotynowi.

W badanych preparatach stwierdzono ponadto występowanie ilwajtu i grafitu, powstałych w toku zastępowania tytanomagnetytu przez asocjację grafitowo-syderytową.

OBJASNIENIE FIGURY

Fig. 1. Część układu Fe-S w niskich temperaturach (według Taylora 1970, zmodyfikowana na podstawie Kulleruda 1968). Wszystkie fazy współwystępują z parą

OBJASNIENIA FOTOGRAFII

Fot. 1. Elektronowy obraz absorpcyjny pentlandytu z lamelkowymi produktami odmieszania $(\text{Fe, Ni})_1(\text{Co, Ni})_2\text{S}_4$. Pow. $\times 460$
białe — piroksen, spękania w pentlandycie, jasnoszare — piroтын, ciemnoszare — pentlandyt z widocznymi jasnoszarymi lamelkami $(\text{Fe, Ni})_1(\text{Co, Ni})_2\text{S}_4$

Fot. 2. Rozmieszczenie FeK_α . Pow. $\times 460$

Fot. 3. Rozmieszczenie CoK_α . Pow. $\times 460$

Fot. 4. Rozmieszczenie SK_α . Pow. $\times 460$

Fot. 5. Rozmieszczenie NiK_α . Pow. $\times 460$

Хенрик КУХА, Адам ПЕСТШИНСКИЙ, Витольд САЛАМОН

ГЕОХИМИЧЕСКО-МИНЕРАЛОГИЧЕСКИЕ ИССЛЕДОВАНИЯ СУЛЬФИДНЫХ МИНЕРАЛОВ ИЗ МАГНЕТИТОВЫХ ГОРНЫХ ПОРОД СЕВЕРО-ВОСТОЧНОЙ ПОЛЬШИ

Резюме

Главным сульфидным минералом в исследуемых породах является пиротин. Присутствует он в двух видоизменённых формах: моноклинной Fe_7S_8 и гексагональной с составом от Fe_9S_{10} до $\text{Fe}_{11}\text{S}_{12}$. Кроме этого обнаружено присутствие смитита $(\text{Fe, Ni})_9\text{S}_{11}$, в котором содержится до 1,2% по весу Ni. Смитит уvolняется в течение процесса окисления моноклинного пиротина. Присутствие никеля связано чаще всего с моноклинным пиротином, в то время как в видоизменениях, которых состав отвечает по атомному составу гексагональному пиротину количество Ni в основном меньше границы обнаружения при помощи электронного микрозонда.

Пентландит присутствует в двух видоизменениях: типической с небольшой примесью кобальта, и аномальной, с большой примесью Co. Кобальтовый пентландит, присутствующий в исходной породе, из-за окисления распался на пентландит нормальный и тиошпинель. Этот распад связан с выделением макинавита. Иногда конечным результатом процесса окисления является образование кобальтового пирита. Пентландит и $(\text{Fe, Ni})_1(\text{Co, Ni})_2\text{S}_4$ могут тоже образоваться в следствие распада (при обнижении температуры) твёрдого раствора моносульфидных соединений богатого Cu, Ni и Co. Этот процесс связан с выделением тальнахита и фаз соответствующих пириту.

В изучаемых препаратах обнаружено тоже присутствие ильванита и графита, которые образовались во время подставления титаномагнетита сидеритово-графитовой ассоциацией.

ОБЪЯСНЕНИЕ К ФИГУРЕ

Фиг. 1. Часть системы Fe-S в низких температурах (по Тайлору 1970, измененная по Куллеруду 1968). Все фазы присутствуют совместно с паром

ОБЪЯСНЕНИЯ К ФОТОГРАФИЯМ

Фото. 1. Электронномикроскопический образ абсорбции пентландита с тонкими пластинчатыми продуктами отделения $(\text{Fe, Ni})_1(\text{Co, Ni})_2\text{S}_4$. Увел. $\times 460$
белые — пироксен (трещины в пентландите), светло-серые — пиротин, тёмно-серые — пентландит, в котором видны светло-серые тонкие пластинки $(\text{Fe, Ni})_1(\text{Co, Ni})_2\text{S}_4$

Фото. 2. Распределение Fe. Увел. $\times 460$

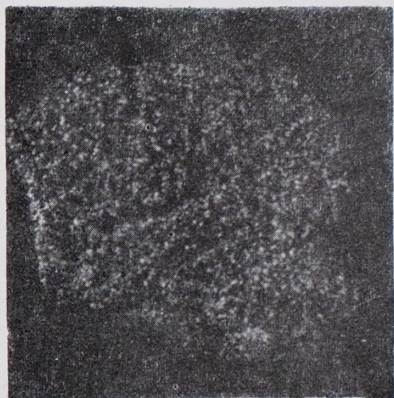
Фото. 3. Распределение Co. Увел. $\times 460$

Фото. 4. Распределение SK. Увел. $\times 460$

Фото. 5. Распределение Ni. Увел. $\times 460$



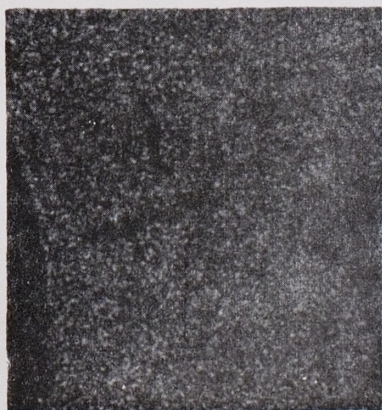
Phot. 1. Electron absorption image of pentlandite containing exsolved lamellae of $(\text{Fe, Ni})_1(\text{Co, Ni})_2\text{S}_4$. Magn. $\times 460$
white — pyroxene, fissures in pentlandite, light-grey — pyrrhotite, dark-grey — pentlandite with light-grey lamellae of $(\text{Fe, Ni})_1(\text{Co, Ni})_2\text{S}_4$



Phot. 2. FeK_α image. Magn. $\times 460$



Phot. 3. CoK_α image. Magn. $\times 460$



Phot. 4. SK_α image. Magn. $\times 460$



Phot. 5. NiK_α image. Magn. $\times 460$

Henryk KUCHA, Adam PIESTRZYŃSKI, Witold SALAMON — Geochemical and mineralogical study of sulphide minerals occurring in magnetite rocks of NE Poland